

Bayesian Human Intention Estimator for Exoskeleton System

Ching-An Cheng, Tzu-Hao Huang, Han-Pang Huang*, *Member, IEEE*

Abstract—The estimation of the human applying torque is critical in many applications, especially in the design of assistive exoskeleton. The most common approaches are the estimation by the inverse dynamics or by the EMG signal. However, the EMG-based torque estimation is not always stable owing to the sweats of skin, the noise from posture change, and the nonlinear mapping between the EMG signal and the human torque. In addition, the estimation based on the dynamic model is unstable in the multi-DOFs system and especially in the existence of exogenous disturbance, such as ground reaction force. Therefore, we propose the Bayesian human intention estimator and the graphical model of human-exoskeleton system to solve these issues. Through the experiments, the proposed method can merge the information from both the EMG signal and dynamic model, and can make the estimated torque more stable.

I. INTRODUCTION

The estimation of the human applying torque in the design of assistive exoskeleton is critical. Most of the exoskeleton systems can be regarded as the human torque amplifier [1]. Since the estimation of human applying torque is difficult in general, various assumptions and models have been proposed during last decades. One approach is to implement force sensor on the exoskeleton to directly measure the interaction force between the operator and the exoskeleton system. The extra force sensors, however, increase the costs and the weight, and decrease the compactness of the exoskeleton system, making the design impractical. Another approach is the model-based method that estimates the human applying torque under the modeling assumption. We roughly classify them into two categories: dynamics model and biosignal model. In [2], they derived the dynamic model of the exoskeleton system and used the positive feedback to increase the sensitivity to the disturbance of the system. The unknown parameters of the dynamic model are calibrated in the experiments [3] and the exoskeleton can amplify any disturbance that comes into the system – even the ground impact force. They claimed “...which does not stabilize, will only make us stronger.” The real question is whether the sensitivity design is stable for all the users regardless of the fitness and whether the calibration can be carried with different subjects efficiently. The stability issue of the sensitivity increasing design was addressed in [4]. They applied the band-pass filter to guarantee the robust stability of the overall system. Further, they proposed a sophisticated smart shoe [5] to estimate the ground reaction force. The dynamic model design is standard in the community of the

control system, but the main drawbacks are the need of the precise modeling and expensive sensors and actuators, not to mention the time delay due to the stability and the causality, since the disturbance comes into the system only when the operator has already moved. The biosignal model alleviates the complexity of the dynamic model, and uses only the biosignals such as the electromyography (EMG) signal or the electroencephalography (EEG) signal to estimate the operator’s intention directly [6-8]. Moreover, EMG and EEG signal activates before the actual movement of the operator and is directly related to the intention of the operator. As the result, a real-time system is possible. Many biosignal models have been proposed, including the linear model, the nonlinear physiology model, and the fuzzy-neural networks, etc. [9, 10]. Due to the low signal-to-noise-ratio (SNR) nature of the biosignals, the methods with only biosignal model, however, can only perform simple or predefined movements. Kawamoto et al. [11] used the clinical database to improve the estimation results, and the others used the finite state machine [12], or hybrid control scheme [13]. The results are not satisfactory for general tasks and the freedom of the movement is limited.

In this paper, we proposed the Bayesian human intention estimator based on the probabilistic graphical model to fuse the information from both the dynamic model and the biosignals model. By human intention, we mean the intended applying torque of the operator, which is denoted as *human applying torque* herein. We treat all the measurements, the biosignals and the states of the dynamics model, as random variables, and use the graphical model to model the joint probability. In machine learning, the graphical model can help the user visualize the structure and the conditional independence of the joint probability, and can simplify the Bayesian reasoning required to perform inference and learning. With the graphical model, the interaction between the biosignal model and the dynamic model is clear, and the Bayesian reasoning can be performed to estimate the operator’s intention. Inheriting the advantage of the biosignal feedback, our system can improve the stability and the causality problem in the system with only dynamic model.

We use the Gaussian process regression to model the conditional probabilities. That is, the conditional probability of the human applying torque given the biosignal, and the conditional probability of the human applying torque given the states of the dynamics. By adopting the Naïve Bayesian assumption, the two conditional probabilities are used to inference the human applying torque with Bayes’ theorem. Consequently, the estimator can adapt itself in different operation zones and trusts the model with more confidence. This can be viewed as a smooth switching estimator. The estimator biases more to the biosignal model when the current SNR is large for instance, and relies on the information

C. A. Cheng and T. H. Huang are with the Department of Mechanical Engineering, National Taiwan University, Taipei, Taiwan, 10617, R.O.C.

H. P. Huang is with the Department of Mechanical Engineering, National Taiwan University, Taipei, Taiwan, 10617, R.O.C. (Corresponding addressee e-mail: hanpang@ntu.edu.tw).

provided by the dynamical model conversely. This method, therefore, takes the advantage of both the models.

The paper is organized as follows. Section II gives the brief reminder of the graphical model and the Gaussian process model. In Section III, we described the framework of the Bayesian human intention estimator, and we show how the Gaussian process can be learned in the experiments. In Section IV, we verify the performance of the proposed model in the experiments, and discuss the results in Section V. Finally, we conclude the contributions and give the future works in Section VI.

For clarity, we summarize the symbols used in this paper in Fig. 1. The bold uppercase denotes the matrix, the bold lowercase denotes the vector, and the others are scalar. $N(\mathbf{x}|\boldsymbol{\mu}, \boldsymbol{\Sigma})$ is the multivariate Gaussian distribution of \mathbf{x} with mean $\boldsymbol{\mu}$ and covariance matrix $\boldsymbol{\Sigma}$. $P(X)$ is the probability of the set X and the $p(x)$ is the probability density function of the random variable x .

II. PRELIMINARIES

In this section, we review the essence of the graphical model and Gaussian process regression that will be used in the following section. Please refer to [14] for the details.

A. Bayesian Networks and Graphical Model

The Bayesian network is known as the directed graphical models in which the links has particular directionality indicated by the arrows. The directed link indicates the factorization of joint probability and each directed link represents the conditional probability. If there is a link that goes from node a to node b , we say a is the parent of b , and b is the child of a . Also, the joint probability can be factorized into $p(a, b) = p(b|a)p(a)$. We say a graph is fully-connected if there is a link between every pair of nodes. In particular, we consider here the directed acyclic graphs, which is the graph with no directed cycles.

One of the features of the directed graphical model is that it represents the conditional independence. This call d-separation, shorted for directed separation, and we give the definition as follows.

Definition 1.

Let A , B , and C be arbitrary non-intersecting sets of nodes in a directed acyclic graph. A path from A to B is blocked if one of the following holds:

- (1) the arrows on the path meet either head-to-tail or tail-to-tail at the node, and the node is in the set C , or
- (2) the arrows meet head-to-head at the node, and neither the node, nor any of its descendants, is in the set C .

If all paths from A to B are blocked observing C , then we say A is d-separated from B by C , and the graph implies that A and B are conditionally independent given C , i.e.

$$P(A, B|C) = P(A|C)P(B|C)$$

Once the factorization of the joint distribution is obtained from the graph, the inference is easy by using Bayes' theorem. Bayes' theorem is commonly used in machine learning algorithms, because it can incorporate the prior knowledge

in the learning. This is called maximum a posteriori estimation (MAP). Given the *a priori* probability, the algorithm returns the model that maximizes the *a posterior* probability after observing the outcomes.

B. Gaussian Process Regression

Gaussian process model is one of the Bayesian machine learning methods, which incorporates the prior knowledge and can inference the probability distribution of the prediction directly. It assumes that the measurement noises η_i , $i=1, \dots, n$, are independent Gaussian random variables $N(\boldsymbol{\eta}|\mathbf{0}, \beta^{-1}\mathbf{I})$, and $\beta > 0$. Under the noise assumption and the linear model assumption, each of the random variables in the model can be modeled by the Gaussian distribution. Therefore, the learning and the inference problems are equal to solving the conditional distribution of the Gaussian random variables.

Given the N training samples $Z = X \times Y$, where $X = \{\mathbf{x}_i \in \mathbb{R}^d, i=1, \dots, N\}$, $Y = \{y_i = f(\mathbf{x}_i) + \eta_i, i=1, \dots, N\}$, and $f: \mathbb{R}^d \rightarrow \mathbb{R}$, the conditional probability is then

$$p(Y|X) = N(Y|\boldsymbol{\Phi}\mathbf{w}, \beta^{-1}\mathbf{I}), \quad (1)$$

where $\mathbf{w} \in \mathbb{R}^{N_H}$, $\phi: \mathbb{R}^d \rightarrow \mathbb{R}^{N_H}$, N_H is the dimension of the feature space and $\boldsymbol{\Phi} = [\phi(\mathbf{x}_1) \ \dots \ \phi(\mathbf{x}_n)]^T$. Assuming that $p(\mathbf{w}) = N(\mathbf{w}|\mathbf{0}, \alpha^{-1}\mathbf{I})$, we know that the marginal probability of $\mathbf{t} := \boldsymbol{\Phi}\mathbf{w}$ is given as $N(\mathbf{t}|\mathbf{0}, \mathbf{K})$, where $\alpha > 0$, $\mathbf{K} = \alpha^{-1}\boldsymbol{\Phi}\boldsymbol{\Phi}^T$ is the Gramian matrix with entries defined as $K_{ij} = k(\mathbf{x}_i, \mathbf{x}_j) := \langle \phi(\mathbf{x}_i), \phi(\mathbf{x}_j) \rangle_H$ the inner product in the feature space. The marginal probability of Y is given by

$$p(\mathbf{y}) = \int p(\mathbf{y}|\mathbf{t})p(\mathbf{t})d\mathbf{t} = N(\mathbf{y}|\mathbf{0}, \mathbf{C}), \quad (2)$$

where $\mathbf{C} := \mathbf{K} + \beta^{-1}\mathbf{I}$ and $\mathbf{y} := [y_1, \dots, y_N]^T$. Finally, the Gaussian process regression model can be obtained by deriving the conditional probability of the new query point \mathbf{x}_{N+1} given the training data \mathbf{y} , that is

$$\begin{aligned} p(y_{N+1}(\mathbf{x}_{N+1})|\mathbf{y}) &= N(y_{N+1} | m(\mathbf{x}_{N+1}), \sigma^2(\mathbf{x}_{N+1})) \\ m(\mathbf{x}_{N+1}) &= \mathbf{k}^T \mathbf{C}^{-1} \mathbf{y} \\ \sigma^2(\mathbf{x}_{N+1}) &= c - \mathbf{k}^T \mathbf{C}^{-1} \mathbf{k} \end{aligned} \quad (3)$$

where $\mathbf{k} = [k(\mathbf{x}_{N+1}, \mathbf{x}_1) \ \dots \ k(\mathbf{x}_{N+1}, \mathbf{x}_N)]^T$, and $c = k(\mathbf{x}_{N+1}, \mathbf{x}_{N+1}) + \beta^{-1}$.

III. BAYESIAN HUMAN INTENTION ESTIMATOR

A. Graphical Model for Exoskeleton System

In this section, we model the joint probability distribution of the exoskeleton system using the graphical model. We use the EMG signal \mathbf{e} for the biosignal model, and the angular position \mathbf{q} , angular velocity $\dot{\mathbf{q}}$, angular acceleration $\ddot{\mathbf{q}}$, and the exogenous disturbance sensor \mathbf{d} for the dynamic model. Note that we do not assume the specific form or the quality of the sensors in this model. The estimator described in the next section can automatically optimize the use of information by adjusting the weighting of different models. Therefore, the

exogenous disturbance sensor can even be simply the foot-switch.

In the proposed method, we made the following assumption.

Assumption.

The total torque $\Sigma\tau$ applied on each joints and the EMG signal \mathbf{e} are d -separated by the human applying torque τ_H , i.e. the random variables are conditionally independent on the true human applying torque.

$$P(\mathbf{e}, \Sigma\tau | \tau_H) = P(\mathbf{e} | \tau_H)P(\Sigma\tau | \tau_H) \quad (4)$$

This assumption is critical to build following graphical model. We argue this is a reasonable assumption, because we know the contribution of the operator into the system once we know the true human applying torque, and the value of the EMG signal becomes irrelevant. The contribution of the EMG signal to the total torque is blocked when the human applying torque is known.

We show the graphical model in Fig. 1, where the green nodes denote the random variables that can be observed in exoskeleton system and the others are the latent random variables. We explain the connection of the graphical model in the following. We assume that the operator is able to track any intended force, so the human applying torque τ_H determines the value of the EMG-signal \mathbf{e} ; The total torque $\Sigma\tau$ applying on each joints is the summation of the human applying torque τ_H , torque provided by the exoskeleton τ_E , and the torque τ_D is passed by the exogenous disturbance \mathbf{d} via the transpose of the Jacobian, which is determined by the angular position \mathbf{q} ; The total torque $\Sigma\tau$ then affects the angular acceleration $\ddot{\mathbf{q}}$ given the current angular position \mathbf{q} and the angular velocity $\dot{\mathbf{q}}$ using the dynamics equation. In summary, the graphical models shows the causal relationship of the dynamics system of the exoskeleton given by

$$\mathbf{M}(\mathbf{q})\ddot{\mathbf{q}} + \mathbf{B}(\mathbf{q}, \dot{\mathbf{q}})\dot{\mathbf{q}} + \mathbf{K}(\mathbf{q}) = \Sigma\tau = \tau_H + \tau_E + \tau_D \quad (5)$$

$$\tau_D = \mathbf{J}(\mathbf{q})^T \mathbf{d}, \quad (6)$$

where $\mathbf{M}(\mathbf{q}) \in \mathbb{R}^{n \times n}$ is the mass matrix, $\mathbf{B}(\mathbf{q}, \dot{\mathbf{q}}) \in \mathbb{R}^{n \times n}$ is the Coriolis matrix, $\mathbf{K}(\mathbf{q})$ is the gravity force, $\mathbf{J}(\mathbf{q})$ is the Jacobian matrix of the current configuration, and n is the number of joints.

From the rules of graphical model, the path from the sensor information of the dynamic model, $\mathbf{d}, \mathbf{q}, \dot{\mathbf{q}}, \tau_E$, to the node of the human applying torque τ_H is unblocked when the angular acceleration $\ddot{\mathbf{q}}$ is observed. In this case, *a posteriori* probability of the human applying torque can be inferred, and the estimated torque is the torque that maximizes the posterior probability. Then again, the EMG signal \mathbf{e} can influence the human applying torque τ_H since it is its descendent.

B. Human Intention Estimation by Bayesian Reasoning

From the graphical model in Fig.1, we can factorize the joint probability distribution into

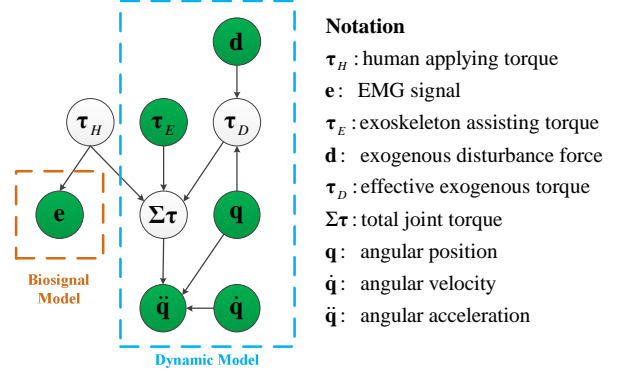


Fig.1. Graphical model of the human-exoskeleton system

$$p(\mathbf{e}, \mathbf{q}, \dot{\mathbf{q}}, \ddot{\mathbf{q}}, \mathbf{d}, \tau_H, \tau_E, \tau_D, \Sigma\tau) = p(\mathbf{e} | \tau_H) p(\Sigma\tau | \tau_H, \tau_E, \tau_D) p(\tau_D | \mathbf{d}, \mathbf{q}) p(\ddot{\mathbf{q}} | \Sigma\tau, \mathbf{q}, \dot{\mathbf{q}}) \cdot p(\tau_H) p(\tau_E) p(\mathbf{d}) p(\mathbf{q}) p(\dot{\mathbf{q}}) \quad (7)$$

The objective is to estimate the conditional probability of the human applying torque given the sensor information,

$$p(\tau_H | \mathbf{e}, \mathbf{q}, \dot{\mathbf{q}}, \ddot{\mathbf{q}}, \tau_E, \mathbf{d}) \sim p(\tau_H | \mathbf{e}) p(\tau_H | \mathbf{q}, \dot{\mathbf{q}}, \ddot{\mathbf{q}}, \tau_E, \mathbf{d}), \quad (8)$$

which is the direct result from Bayes's theorem and the d -separation. The two parts correspond to the biosignal model and the dynamic model respectively. The estimated torque then can be computed as the torque that maximizes the conditional probability.

The two conditional probability distribution are essentially two Gaussian distributions with means μ_{Bio}, μ_{Dyn} and covariance matrices $\Sigma_{Bio}, \Sigma_{Dyn}$,

$$p(\tau_H | \mathbf{e}) = N(\tau_H | \mu_{Bio}, \Sigma_{Bio}) \quad (9)$$

and

$$p(\tau_H | \mathbf{q}, \dot{\mathbf{q}}, \ddot{\mathbf{q}}, \tau_E, \mathbf{d}) = N(\tau_H | \mu_{Dyn}, \Sigma_{Dyn})$$

$$\mu_{Dyn} = \Sigma_{Dyn} (\Sigma_{inv} + \Sigma_D)^{-1} (\mu_{inv} - \tau_E - \mu_D), \quad (10)$$

$$\Sigma_{Dyn} = (\Sigma_H^{-1} + (\Sigma_{inv} + \Sigma_D)^{-1})^{-1}$$

where

$$p(\Sigma\tau | \mathbf{q}, \dot{\mathbf{q}}, \ddot{\mathbf{q}}) = N(\Sigma\tau | \mu_{inv}, \Sigma_{inv}) \quad (11)$$

$$p(\tau_D | \mathbf{q}, \mathbf{d}) = N(\tau_D | \mu_D, \Sigma_D) \quad (12)$$

$$p(\tau_H) = N(\tau_H | \mathbf{0}, \Sigma_H), \quad (13)$$

and $N(\tau_H | \mu_{Bio}, \Sigma_{Bio})$, $p(\Sigma\tau | \mathbf{q}, \dot{\mathbf{q}}, \ddot{\mathbf{q}})$, $p(\tau_D | \mathbf{q}, \mathbf{d})$ are the Gaussian process models of the biosignal, the inverse dynamics, and the exogenous disturbance force, respectively, with the mean and the covariance matrix expressed as in (3), and $p(\tau_H) = N(\tau_H | \mathbf{0}, \Sigma_H)$ is the *a priori* probability of the human applying torque with covariance matrix Σ_H . The conditional probabilities can be easily derived by using the properties of the Gaussian distribution; we leave it for the interested readers due to the limited space.

We use three Gaussian process models in the framework of the proposed Bayesian human torque estimator, and all of them can be learned by MAP in the experiments with the proposed exoskeleton system, which will be detailed in the next section. With the Gaussian process models, the estimator is the MAP solution of the Gaussian distribution that governs all the equations given by

$$p(\boldsymbol{\tau}_H | \mathbf{e}, \mathbf{q}, \dot{\mathbf{q}}, \ddot{\mathbf{q}}, \boldsymbol{\tau}_E, \mathbf{d}) = N(\boldsymbol{\tau}_H | \hat{\boldsymbol{\mu}}_H, \hat{\boldsymbol{\Sigma}}_H)$$

$$\hat{\boldsymbol{\mu}}_H = \hat{\boldsymbol{\Sigma}}_H (\boldsymbol{\Sigma}_{Bio}^{-1} \boldsymbol{\mu}_{Bio} + \boldsymbol{\Sigma}_{Dym}^{-1} \hat{\boldsymbol{\mu}}_{Dym}) \quad (14)$$

$$\hat{\boldsymbol{\Sigma}}_H = (\boldsymbol{\Sigma}_{Bio}^{-1} + \boldsymbol{\Sigma}_{Dym}^{-1})^{-1}$$

$$\hat{\boldsymbol{\tau}}_H := \arg \max p(\boldsymbol{\tau}_H | \mathbf{e}, \mathbf{q}, \dot{\mathbf{q}}, \ddot{\mathbf{q}}, \boldsymbol{\tau}_E, \mathbf{d}) = \hat{\boldsymbol{\mu}}_H \quad (15)$$

From (14), the estimator is the weighted mean of different models by the precision matrices (the inverse of the covariance matrix). Given the current state, the estimator trusts the estimation of the model with the higher precision more. This can only be accomplished by the use of the Gaussian process model. The estimator will consistently bias to one of the models if the traditional regression is used. Also, we note that the online computation of the Gaussian process is fast if the model is linear, since many of the matrix inverses can be pre-computed.

C. Learning the Gaussian Process Regression Model

In this section we give the design of the experiments to learn the Gaussian process models in the proposed Bayesian human torque estimation framework. We want to lessen the hardware requirement of the exoskeleton system by the sophisticated computing. The only required hardware of the proposed estimator is the torque control loop and the position control loop in the exoskeleton system, the biosignal feedback, such as the EMG sensor, and the exogenous disturbance sensor of any form. These are more feasible in practice.

1) The Biosignal Model

To learn the conditional probability $p(\boldsymbol{\tau}_H | \mathbf{e})$, we take use of the joint force sensor in the exoskeleton in the force control loop. In the experiments, the operator is asked to wear the exoskeleton with the EMG sensors. Then the controller of the exoskeleton is set to position regularization mode with different postures, rejecting any disturbance that deviates the mechanism from the current position. The operator is then asked to try to move his leg with arbitrary force, and the computer records the EMG signals and the torque sensing value of the motors. Assuming that the position controller can fix the current position, the Gaussian process model can be performed to learn the mapping between the EMG signal and the torque, that is $p(\boldsymbol{\tau}_H | \mathbf{e})$. Without loss of generality, we use the simple linear model to model the mapping in this paper. Linear model in our experience is sufficient to model relationship in most postures. A more complex model considering the current angular position \mathbf{q} can also be used to obtain a more accurate model, we left it for the future works.

2) The Inverse Dynamics Model

The dynamics of the exoskeleton system can be derived based on Euler-Lagrange equation [15], and it can be identified that the total joint torque is linear in terms of the unknown parameters. Therefore, we can build a linear

Gaussian process model as mentioned in the previous section. In the experiments, the operator is asked to wear the exoskeleton and to relax. The controller of the exoskeleton is set in position control mode to track some predefined trajectories. If the trajectories are sufficient rich [16], then the underlying model can be identifying by the feedback of the torque sensor information and the current state of the exoskeleton to build the model of the conditional probability $p(\boldsymbol{\Sigma}\boldsymbol{\tau} | \mathbf{q}, \dot{\mathbf{q}}, \ddot{\mathbf{q}})$.

3) The Exogenous Disturbance Model

As mentioned in previous section, we do not assume the specific form of the exogenous force sensor. In general, the exogenous disturbance in the exoskeleton system is the ground reaction force, and the force sensor is footpad. The proposed method, however, are not limited to this sensor. Other types of the force sensors, even the footswitch in the worst case, can also be adopted to improve the overall accuracy.

Two scenarios of the experiment are both possible to learn the conditional probability $p(\boldsymbol{\tau}_D | \mathbf{q}, \mathbf{d})$. In the first case, the operator is asked to wear the exoskeleton and relaxed, and the controller of the exoskeleton is set to position regularization with different postures. In each posture, disturbances are injected artificially, and the sensor feedback of the exogenous sensor, torque sensor, and the angular position are used to learn the Gaussian process model.

In the second case, we collect the data based on the learned inverse dynamics model and the measurement of the torque sensor. We design this scenario because it is sometimes more convenient for the experimenter to collect the data while not constraining the movement of the exoskeleton. This is can be done by using the learned model of the inverse dynamics. From the dynamic equation, we know that $\boldsymbol{\tau}_D = \boldsymbol{\Sigma}\boldsymbol{\tau} - (\boldsymbol{\tau}_H + \boldsymbol{\tau}_E)$. Since knowing the human applying torque is generally impossible, we can, however, ask the operator to relax the muscles during the data collection as the trick in the previous experiments. With the learned inverse dynamics model at hand, the noise model in the Gaussian process (1) depends on the prediction of the inverse dynamics model, that is to set $\mathbf{C} = \mathbf{K} + \boldsymbol{\Sigma}_{inv} + \boldsymbol{\beta}^{-1}\mathbf{I}$ in (2). Since the measurement of $\boldsymbol{\tau}_D$ is depending on the estimation of $\boldsymbol{\Sigma}\boldsymbol{\tau}$, the learned Gaussian process model couples with the uncertainty of $p(\boldsymbol{\Sigma}\boldsymbol{\tau} | \mathbf{q}, \dot{\mathbf{q}}, \ddot{\mathbf{q}})$. In summary, during the experiment, the operator is asked to wear the exoskeleton in relaxation. The controller is then set to be position controller to track some predefined trajectories. The computer collects the data of the torque sensor, the exogenous disturbance sensor, and the states of the exoskeleton. The conditional probability $p(\boldsymbol{\tau}_D | \mathbf{q}, \mathbf{d})$ is modeled by the Gaussian regression to learn the mapping from \mathbf{q} and \mathbf{d} to $\boldsymbol{\tau}_D = \boldsymbol{\Sigma}\boldsymbol{\tau} - \boldsymbol{\tau}_E$.

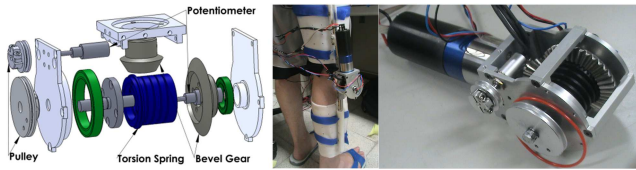


Fig. 2. Exploded view of the proposed backdrivable torsion spring actuator, Knee orthosis, and Backdrivable torsion spring actuator

IV. EXPERIMENTS

In the following experiments, the data acquisition and the controller are implemented on a sbRIO-9642 embedded control and acquisition system (National Instrument Inc.) with sampling rate 250 Hz. To train each Gaussian process model, 6000 training data are sampled uniformly randomly from the recorded data in the previously described experiments. The EMG signals are measured by the active surface EMG electrode with pre-amplifier (B&L Engineering, Inc.) placed on the quadriceps femoris and hamstring muscle, which is later rectified and the DC-component is removed; the states of the exoskeleton systems are calculated by numerical difference; the exoskeleton torque τ_E is measured by the backdrivable spring torsion actuator (BTSA) described below. In addition, all the measurements are filtered by a second-order Butterworth filter with cutoff frequency 15 Hz.

A. Backdrivable Spring Torsion Actuator (BSTA)

In order to collect the sufficient data for building the dynamic model, the biosignal model, and therefore the Bayesian human intention estimator, a BTSA system is constructed using a simple torsion spring, bevel gears, and an actuator. The soft stiffness of the BTSA provides mechanically intrinsic safety and measures the torque between the human and the actuator. Fig. 2 shows the exploded view of the BTSA. Two potentiometers are used. Inside, one potentiometer is inserted into the spring to measure the deflection of the torsion spring, which can be used to calculate the output torque via Hooke's law. The knee angle q is measured by the other potentiometer via the belt transmission between the output joint and the input shaft of the potentiometer. For the specification of the BTSA, please refer to [13]. Finally, we note that with the BTSA the angular position of the output linke can be measured directly, so the effect of the spring can be neglected.

B. Experimental Setting and Procedures

Here, the knee swing motion is used as a toy example to demonstrate the Bayesian human intention estimator for the limited space. In this experiment, the subject was a 31-years-old and healthy male, who was asked to sit on a chair and to drape his foot over the floor. The data collection processes are described in the previous section, although we do not consider the exogenous disturbance sensor in this preliminary stage. By those data, the Bayesian human intention estimator can be learned, and the results suggest the benefit of this approach. Although this is a simple demonstration without the exogenous disturbance, the proposed model can be generalized to any other human motions and situations.

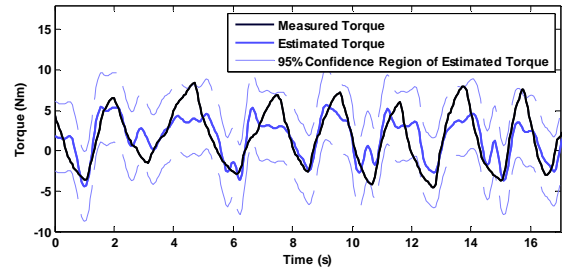


Fig. 3. Measured and estimated human applying torque by biosignal model

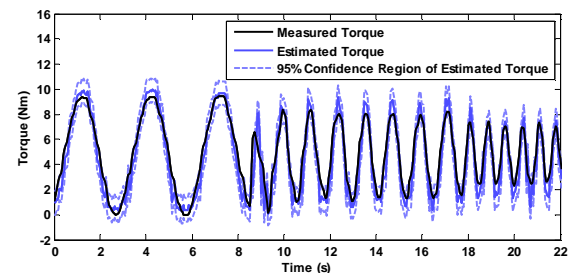


Fig. 4. Measured and estimated torque of dynamic model

In the task for testing the Bayesian human intention estimator, the subject is asked perform voluntary movements with the exoskeleton. In this experiment, there is no assistive torque provided by the exoskeleton. The purpose of this simple example is to demonstrate the characteristics of the proposed estimator.

V. EXPERIMENTAL RESULTS

A. Results of EMG Model

The collected data and the biosignal model are shown in Fig. 3. The solid black line is the measurement, the solid blue line is the estimation, and the dash blue indicated the interval within two standard deviations. It reveals that the variance of the prediction is different in different regions. The regions in which the variance is small mean more reliable prediction. The measured torque and estimated torque have the same tendency, and their values are similar.

B. Results of the Inverse Dynamics Model

Fig. 4 shows the estimated torque of the dynamic model and the measured torque, which are used to verify the inverse dynamics model, since no exogenous disturbance model are used in this simple experiment. Despite of inconsistency in the extreme values, they still share the same tendency, and their values are similar. In addition, the result dynamic model in this experiment is much better than that of the biosignal model in terms of both accuracy and prediction variance, because there is no exogenous disturbance is this experiment, and that the linear biosignal model is only an approximation of the true mapping.

C. Results of Graphical Model

The comparison of the estimation of the Bayesian human intention estimator, the dynamic model, and the biosignal model is shown in Fig. 5. Note that this is the swing motion without the assistance of the exoskeleton, so the exoskeleton torque is caused by the mechanical impedance between the

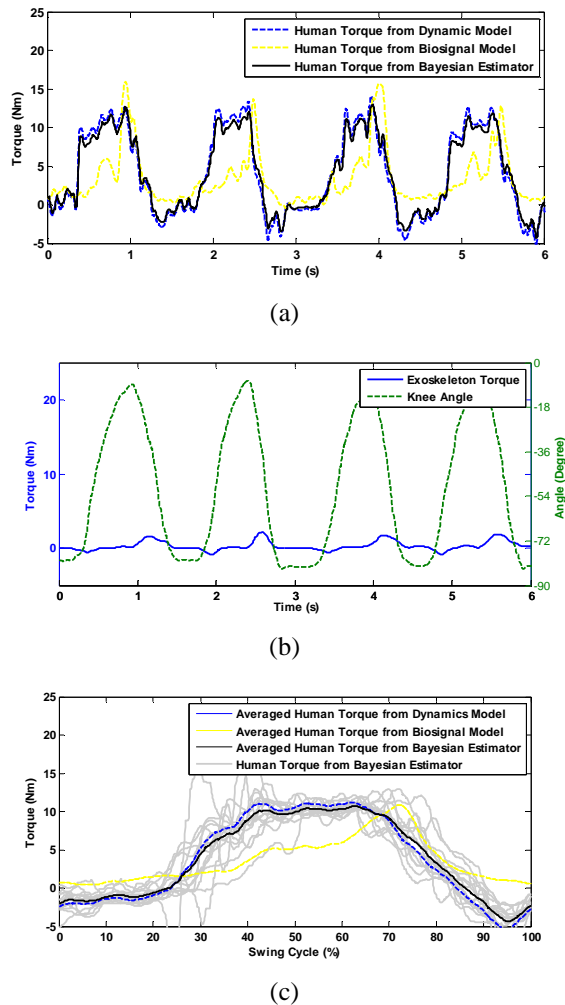


Fig.5. Comparison of the biosignal model, the dynamic model and the Bayesian human intention estimator. (a) the comparison of three models in a trial. (b) the exoskeleton and the angular position. (c) the average performance of the three models.

operator and the exoskeleton. It is not surprising that the estimation of the Bayesian estimator always lies between the estimation of the other two models. Also, since there is no exogenous disturbance in this experiment, the Bayesian estimator bias to the dynamic model almost consistently.

VI. DISCUSSION

In the toy example, we can observe that the Bayesian estimator is indeed the weighted sum of the two models according to prediction confidence. Although the Bayesian estimator biases consistently to dynamic model in this simple demonstration, it is supposed the result will change dramatically once the exogenous disturbance comes in, since the dynamic model fails when the torque generated by the exogenous disturbance in (5) cannot be properly estimated, which is the major disadvantage of the dynamics model. The variance of the prediction of the dynamic model will increase significantly in the presence of the disturbance, e.g. stepping on the floor. In contrast, the biosignal model, despite less accurate, is more consistent in the sense it is not affected by the presence of the exogenous disturbance. Therefore, if the prediction variance induced by both the exogenous disturbance and the dynamic model is at the same level as that

of the biosignal model, the fusion of two models becomes critical and meaningful. In particular, if the exogenous force disturbance is the simple footswitch, which causes largest prediction variance, we suppose the Bayesian estimator may bias to the biosignal model once the exogenous disturbance comes in.

In conclusion, the proposed graphical model for the human-exoskeleton system is general, since it does not limit the source of sensory information. As in the previous discussion, we will implement the exogenous disturbance sensor into our exoskeleton system to verify the proposed estimator in the near future. In particular, we are interested in the case when the exogenous force sensor is just a simple footswitch. Also, the assistive control experiments should be conducted to verify the estimation in tasks such as walking and the climbing stairs.

REFERENCES

- [1] T.-H. Huang, J.-Y. Kuan, and H.-P. Huang, "Design of a new variable stiffness actuator and application for assistive exercise control," in *2011 IEEE/RSJ International Conference on Intelligent Robots and Systems (IROS)*, 2011, pp. 372-377.
- [2] H. Kazerooni and A. Chu, "Biomechanical Design of the Berkeley Lower Extremity Exoskeleton (BLEEX)," *IEEE/ASME Transactions on Mechatronics*, vol. 11, pp. 128-138, April 2006.
- [3] J. Ghan and H. Kazerooni, "System identification for the Berkeley lower extremity exoskeleton (BLEEX)," in *IEEE International Conference on Robotics and Automation*, Orlando, FL, 2006, pp. 3477-3484.
- [4] K. Kong and M. Tomizuka, "Control of Exoskeletons Inspired by Fictitious Gain in Human Model," *Mechatronics, IEEE/ASME Transactions on*, vol. 14, pp. 689-698, December 2009.
- [5] K. Kong and M. Tomizuka, "A Gait Monitoring System Based on Air Pressure Sensors Embedded in a Shoe," *IEEE/ASME Transactions on Mechatronics*, vol. 14, pp. 358-370, June 2009.
- [6] H. Kawamoto, S. Lee, S. Kanbe, and Y. Sankai, "Power assist method for HAL-3 using EMG-based feedback controller," in *IEEE International Conference on Systems, Man and Cybernetics*, Hyatt Regency, Washington, D.C., USA., 2003, pp. 1648-1653.
- [7] T. Hayashi, H. Kawamoto, and Y. Sankai, "Control method of robot suit HAL working as operator's muscle using biological and dynamical information," in *IEEE/RSJ International Conference on Intelligent Robots and Systems*, Edmonton, Alberta, Canada, 2005, pp. 3063-3068.
- [8] J.-Y. Kuan, T.-H. Huang, and H.-P. Huang, "Human intention estimation method for a new compliant rehabilitation and assistive robot," in *Proceedings of SICE Annual Conference 2010*, pp. 2348-2353.
- [9] C. Fleischer and G. Hommel, "A Human-Exoskeleton Interface Utilizing Electromyography," *IEEE Transactions on Robotics*, vol. 24, pp. 872-882, August 2008.
- [10] K. Kiguchi, T. Tanaka, and T. Fukuda, "Neuro-fuzzy control of a robotic exoskeleton with EMG signals," *IEEE Transactions on Fuzzy Systems*, vol. 12, pp. 481-490, August 2004.
- [11] H. Kawamoto, T. Hayashi, T. Sakurai, K. Eguchi, and Y. Sankai, "Development of single leg version of HAL for hemiplegia," in *Annual International Conference of the IEEE Engineering in Medicine and Biology Society*, Minneapolis, 2009, pp. 5038-5043.
- [12] H. Kawamoto and Y. Y. Sankai, "Power Assist Method Based on Phase Sequence Driven by Interaction between Human and Robot Suit," in *IEEE International Workshop on Robot and Human Interactive Communication*, Kurashiki, Okayama, Japan, 2004, pp. 491-496.
- [13] T.-H. Huang, H.-P. Huang, C.-A. Cheng, J.-Y. Kuan, P.-Y. Lee, and S.-Y. Huang, "Design of a new hybrid control and knee orthosis for human walking and rehabilitation," in *IEEE/RSJ International Conference on Intelligent Robots and Systems Vilamoura-Algarve*, Portugal, 2012, pp. 3653-3658.
- [14] C. M. Bishop, *Pattern Recognition and Machine Learning* Springer, 2007.
- [15] B. Siciliano and O. Khatib, *Springer Handbook of Robotics*: Springer, 2008.
- [16] P. Ioannou and B. Fidan, *Adaptive Control Tutorial* SIAM, 2006.